Materials Letters 65 (2011) 2676–2679

Contents lists available at ScienceDirect

Materials Letters

journal homepage: www.elsevier.com/locate/matlet

Enhancement on the afterglow properties of $Sr_2MgSi_2O_7$: Eu^{2+} by Er^{3+} codoping

Haoyi Wu, Yihua Hu *, Li Chen, Xiaojuan Wang

School of Physics & Optoelectronic Engineering, Guangdong University of Technology, Waihuan Xi Road No. 100, Guangzhou 51006, PR China

ARTICLE INFO

Article history:
Received 3 January 2011
Accepted 21 May 2011
Available online 30 May 2011

Keywords:
Luminescence
Optical materials and properties
Phosphors
Thermoluminescence

ABSTRACT

The $Sr_{1.99}MgSi_2O_7$: $Eu^{2+}_{0.01}$, and $Sr_{1.97}MgSi_2O_7$: $Eu^{2+}_{0.01}$, $R^{3+}_{0.02}$ (R: Dy, Er) are synthesized via high temperature solid-state reaction. The sample without codoping shows the highest luminescent efficiency, leading to the strongest emission intensity. Both Dy^{3+} and Er^{3+} enhance the afterglow properties. Compared with Dy^{3+}, sample doped with Er^{3+} shows a longer afterglow duration because of a deeper trap and it may be the optimum codopant for $Sr_2MgSi_2O_7$: Eu^{2+} long afterglow phosphors.

1. Introduction

Afterglow refers to the light emission of the phosphors that persists for a duration after excitation. Because of this characteristic, materials with long afterglow have been used in many aspects, such as watch dials, luminous paints, traffic signs and emergency signage etc. [1,2]. The traditional phosphors are the sulfides doped with Cu^+, which have been used for many years. However, the emission of these phosphors is not bright enough and the afterglow is not maintained for more than few hours. Rare earth (Re) doped aluminates such as Sr_2AlO_4: Eu^{2+}, Dy^{3+}, with high brightness and long afterglow duration, have been developed for more than 10 years after discovery [3,4]. However, the luminescent properties of aluminates are degraded when exposed to water and hence their usage is limited. Simultaneously, Re doped silicates have been found to show long afterglow [5,6]. Compared with the aluminates, the silicates possess of comparable luminescent properties and better chemical stability. Therefore, they potentially have a better commercial application.

One of the research focuses is to enhance the duration of the afterglow. It is reported that codoing with Dy^{3+} improves the afterglow duration of $Sr_2MgSi_2O_7$: Eu^{2+} [7], which is regarded as an important silicate-based phosphors for the long afterglow usage. Dorenbos [8] provided a scheme that showed the levels of different lanthanides. According to his mechanism which is based on the electron trapping, Nd^{3+}, Ho^{3+} and Er^{3+} should have a similar effect as Dy^{3+} on the enhancement of afterglow because their 4f of divalent states locate at the approximate positions. However, his model cannot explain the afterglow phenomenon of Eu^{2+} single dope materials. Enhancement of Nd^{3+}, Ho^{3+} on the afterglow of $Sr_2MgSi_2O_7$: Eu^{2+} has been observed in the previous researches [9,10]. They are not as superior as the influence of Dy^{3+}. This implies somewhat rationality of this model which however, should be improved. In the present work, the enhancement of Er^{3+} will be presented by the comparison with that of Dy^{3+} which seems to be the optimum for the long afterglow, and the relative mechanism will be discussed.

2. Experimental procedure

The samples $Sr_{1.99}MgSi_2O_7$: $Eu^{2+}_{0.01}$ (denoted as SE), and $Sr_{1.97}MgSi_2O_7$: $Eu^{2+}_{0.01}$, $R^{3+}_{0.02}$ (R: Dy, Er; denoted as SED and SEE, respectively) were synthesized via high temperature solid-state reaction. The raw materials $SrCO_3$, MgO, SiO_2, Eu_2O_3, Dy_2O_3 and Er_2O_3, all of analytical purity, were employed and 8 mol% of H_3BO_3 was added as flux. Initially, the raw powders were weighed according to the nominal compositions and then the powders were mixed and milled thoroughly for 2 h. After that the powder mixtures were sintered at 1250 °C for 2 h in a weak reducing atmosphere (95% N_2 + 5%H_2). At last the nominal compounds were obtained after cooling down.

Phase identification of the powders was carried out by powder x-ray diffraction (XRD) using a diffractometer with Cu Kα irradiation ($\lambda = 1.5406$ Å) at 36 kV tube voltage and 20 mA tube current. The morphology of the samples was studied via scanning electron microscope (SEM) using a Hitachi S3400N microscope. The excitation and emission spectra of all the samples were recorded by a Hitachi F-7000 fluorescence spectrophotometer. X-ray Photoelectron Spectroscopy (XPS) was carried using a Thermo-VG Scientific Escalab 250. The decay curves were measured by a GFZF-2A single-photon counter system. Prior to the measurement, all samples were excited by a fluorescence lamp for 1 min. The thermoluminescence (TL) curves were recorded using a FJ427A1 thermoluminescent dosimeter. The heating rate was 1 K s^{-1} for

* Corresponding author. Tel.: +86 20 39322262; fax: +86 20 39322265.
E-mail address: huyh@gdut.edu.cn (Y. Hu).

0167-577X/$ – see front matter © 2011 Elsevier B.V. All rights reserved.
doi:10.1016/j.matlet.2011.05.079

each sample. All the samples were excited by a fluorescence lamp for 1 min and the measurement started with 15 min delay time.

3. Results and discussion

As shown in Fig. 1(a), SE, SED and SEE exhibit the identical diffraction patterns. They can be indexed to tetragonal $Sr_2MgSi_2O_7$ structure with the space group P-421m (No. 113) according to JCPDF card no. 75–1736. No other phase is observed significantly. Eu^{2+}, Dy^{3+} and Er^{3+} ions are regarded to occupy the Sr^{2+} sites in the matrix because of the similar covalent radius (Sr^{2+}: 195 pm, Eu^{2+}: 198 pm, Dy^{3+}: 192 pm, Er^{3+}: 189 pm). The morphology of SED and SEE is exhibited in Fig. 1(b) and (c) respectively. Both samples are particles within the grain size of 1–50 μm. Small amount of the doping has significant influence on the neither the structure nor the morphology of the samples.

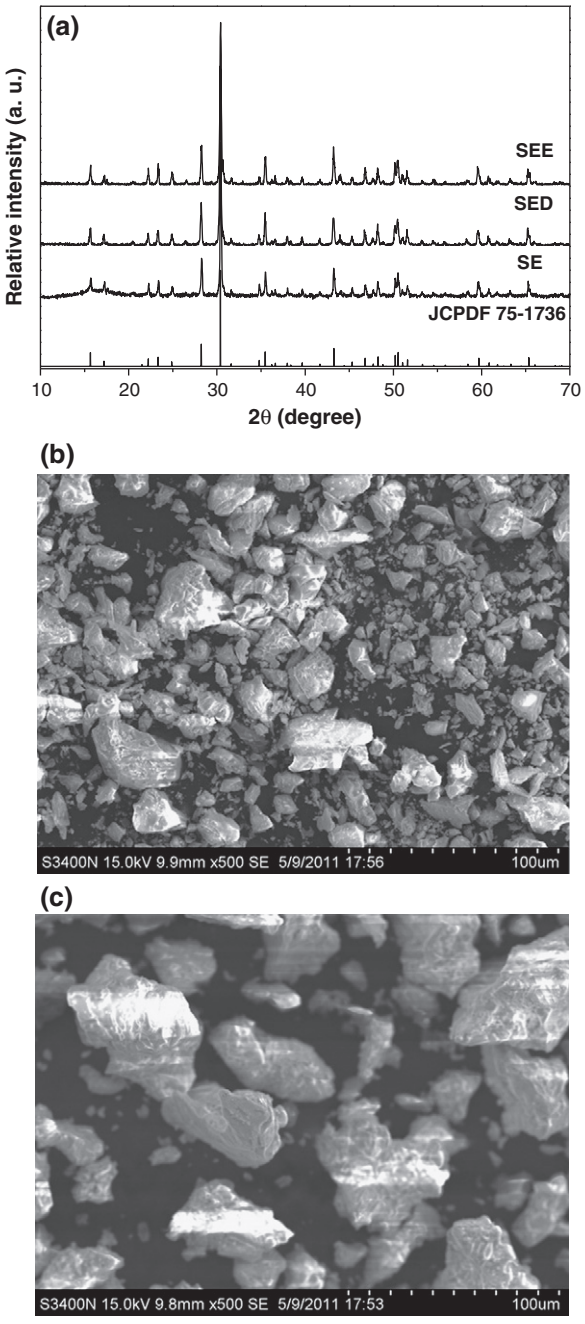

Fig. 1. (a) XRD patterns of the samples (b) SEM of SED (c) SEM of SEE.

The emission and excitation spectra are shown in Fig. 2(a) and (b). All samples show the similar emissions centering around 468 nm. These emissions attribute to the $4f^6 5d$ to $4f^7$ transition configuration of Eu^{2+} ions. No other emission is observed, indicating that Dy^{3+} and Er^{3+} ions do not show emissions significantly. The excitation spectra are also similar, showing more than three absorption bands from 250 nm to 400 nm. The phosphors can absorb the ultraviolet light efficiently. The emission intensity of SE is about three times stronger than those of SED and SEE, resulting from greater luminescent efficiency of SE. The Dy^{3+} and Er^{3+} ions do not influence the color of the phosphors but the luminescent intensity.

XPS of SED and SEE was performed and the results are shown in Fig. 2(c) and (d), respectively. A weak peak centered around 1299 eV of SED can be designated to the 3d electronic state of Dy^{3+} [11] meanwhile a weak peak centered around 168 eV of SEE can be designated to the 4d electronic state of Er^{3+} [12]. Although spectra do not show emissions from Dy^{3+} and Er^{3+}, the results of XPS indicate the existence of Dy and Er in the matrix.

The decay curves of the samples are shown in Fig. 3. As shown in Fig. 3(a), SE exhibits an obvious afterglow phenomenon. This demonstrates that traps which induce the afterglow have already existed even without Re^{3+} doping. When the phosphors are doped with Dy^{3+} or Er^{3+}, the afterglow intensity is strongly enhanced. Furthermore, the duration of the afterglow is prolonged since the intensity of SED or SEE is stronger than the one of SE all the time. On the other hand, the decay curves of SED and SEE coincide very well. Their decay trends are very close to each other. The 600 s initial and last data of decays are shown in Fig. 3(b) and (c), respectively. During the initial 600 s, the decay curves of SED and SEE overlap each other and it is difficult to distinguish their difference, whereas they have splitted during the last 600 s. Decay possessed of SEE is a little stronger than that possessed of SED.

Since the decay process contains the rapid-decaying process and the slow-decaying process, the decay curves of the samples can be also evaluated by fitting into double exponential equation which reflects the trend of the decay. The form of the equation is as follows:

$$I = I_{01}\exp\left(-\frac{t}{\tau_1}\right) + I_{02}\exp\left(-\frac{t}{\tau_2}\right) \quad (1)$$

where I represents the phosphorescent intensity. I_{01} and I_{02} are constants. τ_1 and τ_2 are decay constants, deciding rates for the rapid and the slow exponentially decay components respectively. The fitting results of slow-decaying process parameters τ_2 are 116.5 s, 526.4 s and 548.5 s corresponding to SE, SED and SEE, respectively. These results imply that afterglow duration of SEE is a little longer than that of SED since τ_2 which reflects the slow exponentially decay component, has a greater value. This conforms to the trend of the decay curves.

In general, the afterglow of phosphors is considered to be generated by the detrapped carriers which recombine in the luminescent centers accompanied by the delay emission, hence the traps which induced by the lattice defects in phosphors play an important role on the afterglow. TL provides a possible method to investigate these traps. As shown in Fig. 4, SE, SED and SEE present a broad TL band peaking at 73 °C, 88 °C and 91 °C, respectively. The locations of the glow peaks indicate that the sequence of the trap depth should be SE<SED<SEE, because the higher temperature the peak locates, the greater activation energy is needed for detrapping. The glow intensity has the similar sequence. Moreover, intensities of SED and SEE are much stronger than that of SE, indicating that the formers have a higher ability of trapping carriers.

The trap depth of the samples can be obtained by fitting experimental TL data to the general order kinetics formula and then